OPTICS: Human Activity-Aware Integrated Optical Wireless Communication and Sensing

Yue Zhang, Wei Wang, Nan Cen
Department of Computer Science
Saint Louis University
St. Louis, Missouri, USA
Email:{yue.zhang.5, wei.wang.5, nan.cen}@slu.edu

IEEE INFOCOM 2025 - IEEE Conference on Computer Communications | 979-8-3315-4305-1/25/$31.00 ©2025 IEEE | DOI: 10.1109/INFOCOM55648.2025.11044687

***Abstract*—Optical Wireless Communication (OWC) is emerging as a promising complementary technology for 6G and beyond, with a significant increase in research focused on optical-based communication and sensing in recent years. However, until now, these two applications are still being investigated separately within the same system, which hinders further performance improvements. Moreover, the high directionality and low penetration characteristics of optical signals can lead to frequent interruptions caused by human activities, posing significant challenges for both communication and sensing tasks.**

In this paper, we present OPTICS: an Optical-based Integrated Communication and Sensing (OPTICS) system that seamlessly integrates optical wireless communication and sensing to create a synergistic benefit for both functions. To achieve this, OPTICS analyzes the received signal patterns to identify human activities and dynamically modifies the transmitted optical signals to simultaneously preserve communication quality and enhance human activity recognition. We implemented OPTICS using off-the-shelf devices and conducted extensive evaluations under various real-world scenarios. The results demonstrate that OPTICS can effectively improve original OWC reliability and throughput while achieving up to 99.1% accuracy in human activity recognition.

***Index Terms*—Integrated Optical Wireless Communication and Sensing, Human Activity Recognition**

I. Introduction

Optical Wireless Communication (OWC) is an innovative wireless communication technology that utilizes light as the transmission medium. Compared to Radio Frequency (RF) communication technologies, OWC offers numerous advantages, including (i) higher data rates [1]–[3], (ii) no interference to RF communication [4]–[6], (iii) robust to multipath effect [7]–[9], and (iv) low implementation cost and simple frontends [10]–[12]. These benefits make OWC a necessary complementary wireless technology to RF communication for 6G and beyond. With the advances in OWC techniques, optical-based wireless sensing techniques have also been proposed for human activity recognition [13]–[15]. Unlike traditional sensor-based approaches, these techniques do not require attaching sensors to human targets, thus enhancing user convenience and enabling unobtrusive monitoring. Furthermore, by utilizing existing light signals as the sensing medium, no additional interference is introduced to conventional RF-based communication systems.

Although existing OWC and optical-based wireless sensing techniques have demonstrated their effectiveness, they are normally treated as two different topics and investigated independently within the same system or application scenarios (e.g., smart office [12], [16], smart home [17], [18], smart building [17], [19], etc.), which limits their potential for performance improvements. Moreover, several critical challenges still remain unsolved for OWC and optical-based wireless sensing tasks. **First,** due to the high directionality and low penetration characteristics of light, OWC signals can be blocked by the human body. As a result, human activities can easily disrupt the original OWC transmission. To mitigate this issue, one potential solution is to deploy many Re-configurable Intelligent Surfaces (RIS) [20]–[22] to redirect the light beam to the receiver. However, RIS components are typically expensive and require expert installation, making this solution inefficient for addressing the blockage problem caused by dynamic and irregular human activities. **Second,** optical-based wireless sensing techniques normally require multiple light sources or receivers to work together for human activities [23]–[26]. These approaches not only need extra hardware components but also rely on relatively complex deep-learning models for signal processing and human activity recognition, which limits the wide adoption of these techniques. Given that both OWC and optical-based wireless sensing techniques use light as a medium, in this paper, we ask this question: ***Can we seamlessly integrate OWC and optical-based wireless sensing to create a win-win situation for both sensing and communication tasks?***

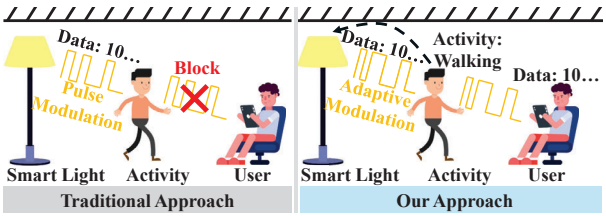

Fig. 1: Comparison between conventional OWC and OPTICS.

To answer this question, we introduce **OPTICS:** an **Optical-based Integrated Communication and Sensing (OPTICS)** system that not only preserves the original optical wireless communication but also supports accurate human activity recognition at the same time. The **core idea** behind OPTICS is to adaptively modify and control the transmitted optical signals according to human activities to enhance both communication reliability and activity recognition accuracy.

As shown in Figure 1, the conventional optical wireless communication system (smart light) uses the commonly-used Variable Pulse Position Modulation (VPPM) scheme [27] to communicate with the user. However, the transmitted signals can be easily blocked by human activities. In contrast, OPTICS can recognize human activities and dynamically modulate the transmitted signal to successfully deliver data to the end user. Moreover, based on the data delivery results, OPTICS can further adjust the transmitted signal to significantly enhance communication reliability and activity recognition accuracy. To build this system, we mainly encounter three challenges:

I. How to achieve human activity recognition for both known and unforeseen activities? Recognizing corresponding human activities that cause signal blockage is essential for adjusting transmitted light signals. However, this task is very challenging. **First,** unlike traditional RF sensing approaches [28]–[30], where signals can partially penetrate obstacles, optical signals are completely blocked by human activities, which makes it difficult to analyze the received signals for activity recognition. **Second,** human activities are highly randomized and inconsistent [31]. Using pre-trained models for human activity recognition may reduce recognition accuracy. More importantly, different from traditional sensing systems [24]–[26], [29], [30], OPTICS relies on accurate human activity recognition to adjust OWC transmissions. Failure to recognize human activities will significantly reduce communication reliability. To overcome these challenges, we conducted extensive experiments and found that the signal blockage patterns detected by the receiver are highly correlated with human activities. By leveraging this interesting feature, we introduce a novel Optical-Signal-Based Hybrid Human Activity Recognition Model (H-HAR) to recognize both known and unforeseen activities at the same time.

II. How to preserve the original OWC transmission when Line-of-Sight (LoS) paths are blocked by human activities? Due to the high directionality and low penetration characteristics of optical signals, human activities can block the OWC transmission, which significantly reduces communication reliability. To overcome this challenge, OPTICS leverages the feature of the current variable pulse position modulation scheme used in the OWC system. Specifically, according to human activities, OPTICS generates and dynamically adjusts the width of the pulse signal to avoid the potential blockage caused by human activities. Since the receiver demodulates the optical signal by analyzing the position of the pulse in a symbol, partially recognized pulses are still sufficient for correct demodulation. By adaptively adjusting the pulse width, OPTICS preserves the original OWC transmission without being affected by human activities.

III. How to determine the optimal OWC signal to achieve higher throughput when Line-of-Sight (LoS) paths are blocked by human activities? To improve communication reliability when LoS paths are blocked by human activities, we can maximize the width of the light pulse to ensure that the receiver can always detect the light signal. However, increasing the pulse width will result in a longer symbol duration, which negatively impacts communication throughput. To address this tradeoff, one possible solution is to build a fixed table to map optimal light pulse with different human activities. However, due to the uncertainty and irregular characteristics of human motions and wireless channels, a fixed table cannot adapt to dynamically changing conditions. To overcome this challenge, OPTICS introduces a novel Adaptive Intelligent Control (AIC) to dynamically update the pulse width based on the transmission status (i.e., bit error rate and data rate) of the OWC. For instance, if the bit error rate is too high, the pulse width will be increased. Conversely, if the data rate is low, the pulse width will be reduced.

Our major contributions are summarized as follows:

- To the best of our knowledge, OPTICS is the ***first work*** that in-depth explores the potential to seamlessly integrate OWC and optical-based wireless sensing to create a win-win situation for both communication and sensing tasks, including preserving original OWC transmission, improving communication reliability and throughput, and accurately recognizing human activities.
- To the best of our knowledge, OPTICS is the ***first work*** that discovers and models the signal blockage features associated with human activities. It answers the question of how to dynamically adjust the optical signals to perform simultaneous communication and sensing.
- We implement OPTICS using off-the-shelf devices and extensively evaluate its performance under various real-world scenarios. The evaluation results demonstrate the effectiveness of our design.

II. Preliminary Analysis and Observations

In this section, we first discuss the impact of human activities on the current OWC system. Then, we analyze existing optical-based human activity recognition approaches and explore a novel research direction - using data-level patterns to recognize human activities. At last, we conduct experiments to prove the potential of our research direction.

A. Impacts of Human Activities on Current OWC Systems

To conduct optical wireless communication (OWC), the OWC transmitter modulates the light intensity to embed the data bits into the light. To demodulate the transmitted data, a Photo Detector (PD) is leveraged by the receiver to directly detect the light intensity and convert the corresponding variations into data bits. However, since optical signals can be easily blocked by human activities, communication reliability and throughput of OWC are severely decreased in crowded areas. To prove our analysis, we deployed the OWC system at different locations to study the performance degradation caused by human activities. As shown in Table I, compared to the ideal scenario (lab), the throughput of OWC significantly decreased by 13%, 29%, and 70% in the office, mall, and classroom, respectively. This is because these scenarios are normally crowded and human activities block the optical signal transmitted from the OWC transmitter. This observation emphasizes the urgent need to adaptively adjust the OWC signal to ensure reliable and high throughput communication.

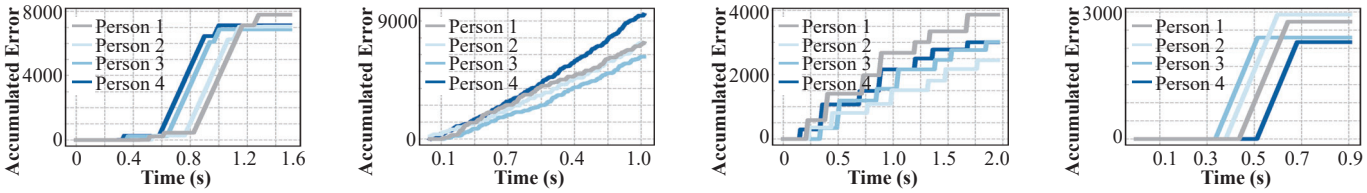

(a) Walking (b) Waving Arm (c) Kicking (d) Running

Fig. 2: Accumulated OWC bit errors caused by human activities. Different activities and persons show significantly different patterns.

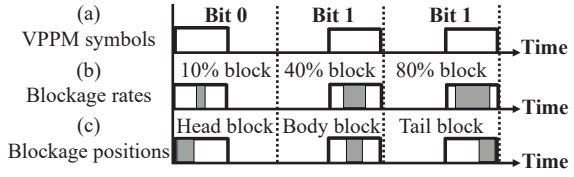

Fig. 3: VPPM Symbols with Different Blockage Rates and Positions

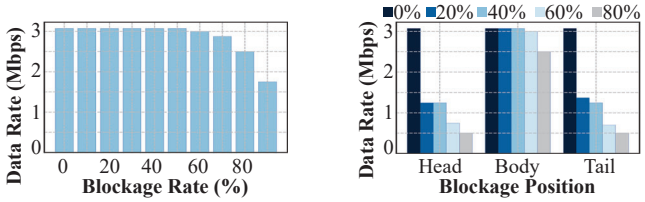

(a) OWC Data Rates vs. Blockage Rates (b) OWC Data Rates vs. Blockage Positions

Fig. 4: OWC Data Rates under Different Blockage Settings

B. Analysis of Optical-based Human Activity Recognition

Current optical-based human activity recognition approaches mainly leverage the shadows introduced by human activities to distinguish different activities [23]–[25], [32], [33]. Specifically, as the light is blocked by the human body, it casts a silhouette. These shadows can serve as a projection of human activities, enabling the recognition of different activities. For example, StarLight [32] leverages the light emitted from ceiling LED panels to reconstruct fine-grained user skeleton postures. Meanwhile, Aili [33] utilizes table lamp LED panels to reconstruct a 3D hand skeleton. Although current approaches demonstrate the potential of using optical signals for human activity recognition, they require the deployment of many transmitters or receivers in a relatively small space, making these methods impractical for real-world scenarios. Moreover, these approaches mainly focus on achieving high activity recognition accuracy. The question of "how to leverage activity recognition results to improve the performance of OWC" remains unanswered.

Instead of focusing on the shadow, we turn our attention to the unique patterns of the received data in the OWC system. Specifically, when human activity occurs between the OWC transmitter and receiver, part of the human body will ***intermittently*** block the optical signal. As a result, the receiver will observe short and recurrent disruptions. In this work, our **key assumption** is that ***the short and recurrent disruption detected by the receiver will form various patterns for different activities.*** We can analyze these unique patterns to recognize human activities.

Figure 2 shows the accumulated bit errors of OWC transmissions caused by different human activities, including walking, waving arm, running, and kicking. It is important to note that during these experiments, we only deployed a single OWC transmitter and receiver. As observed from the figure, different activities and individuals exhibit significantly different patterns. This observation supports our assumption and motivates us to recognize human activities by distinguishing the unique patterns in the received data. These experiments also demonstrate the feasibility of recognizing human activities using a limited number of OWC devices.

	Lab	Office	Mall	Classroom
Throughput (Mbps)	3	2.61	2.13	0.89

TABLE I: OWC Throughput in Different Scenarios

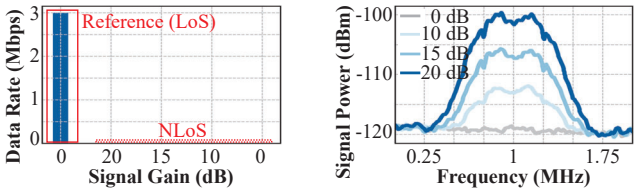

(a) Data Rates (b) Received Signal Power

Fig. 5: Data Rate and Received Signal Power in NLoS Scenarios

C. Experiments and Observations on OWC Systems

In the OWC system, Variable Pulse Position Modulation (VPPM) is one of the most commonly used modulation schemes defined in IEEE 802.15.7 [34] to achieve reliable and high-throughput communication. VPPM embeds data bits by changing the position and width of the light pulse. To demodulate the optical signal, the receiver detects the head and tail of the light pulse to extract the transmitted data bits. According to this demodulation scheme, theoretically, even if parts of the light pulse are blocked, the receiver should still be able to demodulate the transmitted signal correctly. In other words, as long as human activity does not block the entire optical pulse, the reliability and throughput of the OWC should remain unaffected.

To prove our analysis, we first define the blockage rate as the ratio of the length of the blocked portion of the optical signal pulse to the total length of the original signal pulse. Then, we conducted experiments to study the relationship between different blockage settings and their corresponding data rates.

• **Different Blockage Rates**: In Figures 3 (a) and (b), we modify VPPM signals with different blockage rates. Figure 4 (a) shows OWC data rates under different blockage rates. As we can observe from this figure, the data rates are relatively stable even if 60% of the optical pulses are blocked. When the blockage rate reaches 80%, the corresponding data rate is still nearly $2.5 Mbps$. **In summary**, the OWC transmissions are relatively robust under different blockage rates.

• **Different Blockage Positions**: In Figure 3 (c), we modify VPPM signals with different blockage positions (the head, body, and tail of the optical pulse). As we can see from Figure 4 (b), the blockage at the head and tail of the signal negatively affects the OWC data rates. This is because the OWC receiver cannot accurately locate the position of the optical pulse to conduct demodulation. Conversely, body blockages have no significant effect on OWC data rates. This observation provides valuable **insight** to guide our design: we should develop novel approaches to help the OWC receiver accurately locate the optical pulses when head or tail blockages occur.

Besides the above experiments, we also study the impact of the NLoS transmissions in OWC systems. Specifically, due to the high directionality and low penetration characteristic of the optical signal, OWC mainly relies on the Line-of-Sight (LoS) transmission. As shown in Figure 5 (a), the throughput of OWC in the LoS scenario is $3Mbps$. In contrast, even when the transmission power is increased, the throughput of OWC in the NLoS scenario still drops to $0Mbps$. This is because the Signal-to-Noise Ratio (SNR) of the received signal in the NLoS scenario is too low for the receiver to conduct demodulation. Interestingly, as shown in Figure 5 (b), the OWC receiver is sensitive enough to detect the variations in the ambient light noise introduced by changes in transmission power. This observation provides another valuable **insight**: even if the LoS path is blocked by human activities, the NLoS path may still assist the OWC transmission.

Based on the above analysis, experiments, and observations, in OPTICS, we extract the unique data patterns of the received signal to recognize human activities. Moreover, according to human activities, we adaptively modify the pulse width of the optical signal and the transmission power to support reliable and high throughput optical wireless communication.

III. System Overview

The objective of OPTICS is to seamlessly integrate sensing and communication using optical signals and create a win-win situation for both sensing and communication tasks: preserving original OWC transmission, improving communication reliability and throughput, and accurately recognizing human activities. Figure 6 shows the overall architecture of our system, which consists of four key components: **(i) Optical-Signal-Based Hybrid Human Activity Recognition Model (H-HAR)**, **(ii) Adaptive Intelligent Control (AIC)**, **(iii) Activity-Aware Dynamic & Adaptive Modulation/Demodulation (ADAM)**, and **(iv) Blockage-Resilient Synchronization (BRS)**.

• **Optical-Signal-Based Hybrid Human Activity Recognition Model (H-HAR)**: The H-HAR is designed to identify various human activities by discovering the patterns of the received optical signals. To address the challenges posed by highly randomized and irregular human activities and to ensure sensing accuracy, a hybrid supervised learning and unsupervised learning model is designed to identify the commonly known human activities and the irregular unforeseen activities.

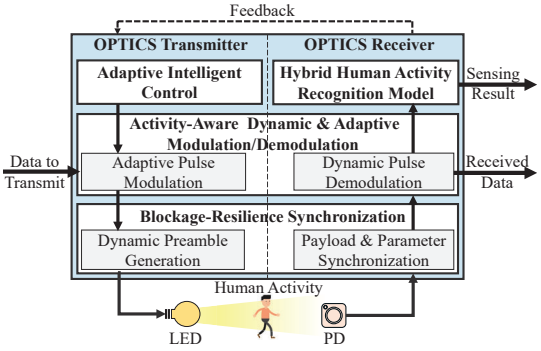

Fig. 6: OPTICS Design Overview

• **Adaptive Intelligent Control (AIC)**: The AIC is designed to dynamically determine the pulse width of the optical signal to achieve high reliability and throughput in OWC. To accomplish this, the AIC adaptively searches the potential pulse widths and uses an optimal parameter determination algorithm to modify the transmitted optical signals. Specifically, based on the current transmission status (i.e., data rate and bit error rate) and human activities, the AIC determines an appropriate pulse width range, where all pulse width in the range can maintain ongoing communication when varying human activities occur. Then, an optimal pulse width determination algorithm finds the optimal pulse width in the determined range.

• **Activity-Aware Dynamic & Adaptive Modulation/ Demodulation (ADAM)**: The design purpose of the Activity-Aware Dynamic & Adaptive Modulation/Demodulation (ADAM) is to accurately modulate and demodulate the optical signal according to the optimal pulse width results determined by AIC. Specifically, the ***adaptive pulse modulation*** at the transmitter will modulate the transmitted signal according to the optimal pulse width to ensure reliable and high throughput communication. Then, at the receiver, an ***dynamic pulse demodulation*** method precisely decodes the received signals during dynamic human activities.

• **Blockage-Resilient Synchronization (BRS)**: The Blockage-Resilient Synchronization (BRS) is designed to synchronize the transmitter and receiver in dynamic channel conditions to avoid the demodulation failure caused by blockage and pulse width change. To achieve this, we introduce an innovative ***dynamic preamble generation*** module to update the optimal pulse width information to the receiver and help it determine the location of the payload. At the receiver, ***payload & parameter synchronization*** module is proposed to seamlessly obtain the updated pulse width and simultaneously distinguish the preamble and payload.

IV. Detailed Design

A. Hybrid Human Activity Recognition Model (H-HAR)

In Figure 7, we first introduce a novel ***Hybrid Human Activity Recognition Model (H-HAR)*** to recognize human activities. The design principle of the H-HAR is to identify distinct received optical signal patterns caused by various human activities. In practice, achieving accurate human activity recognition is very challenging due to the random

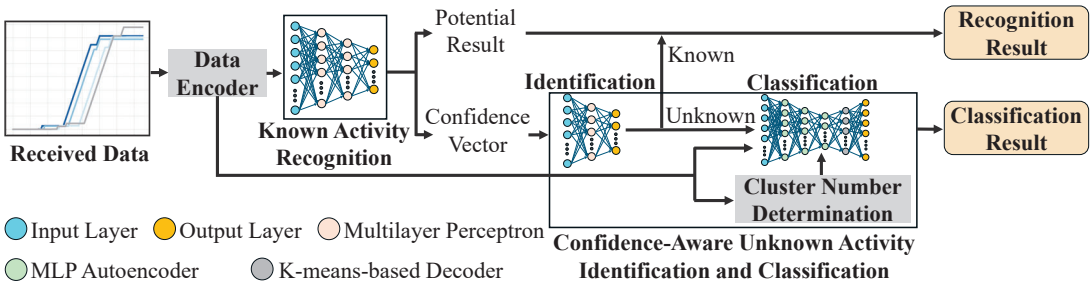

Fig. 7: Optical-Signal-Based Hybrid Human Activity Recognition Model (H-HAR)

and inconsistent nature of human activities across different individuals, especially when unforeseen activities occur. To address this challenge, we propose H-HAR, a hybrid supervised learning and unsupervised classification model. H-HAR mainly consists of two parts: **(i)** known activity recognition and **(ii)** confidence-aware unknown activity identification.

1) Known Activity Recognition: To recognize the known activity, we design a supervised learning-based multilayer perceptron neural model to extract informative features from the received data pattern. We consider common and natural human activities, such as walking, waving arms, kicking, and running, as known activities for model training. To expedite the learning process, we propose a data encoder to reduce the dimension of the received data bit stream. This encoder groups successive received bits into segments of size s, and then counts the number of successfully and unsuccessfully received bits within each segment. The resulting statistics are used as new features for model training. The output of this module is a confidence vector, which indicates the likelihood of all pre-trained known activities while the activity with the highest value is the final result. In practice, we need to note that the parameter s is tunable to allow flexible adjustment based on data size and transmission speed.

2) Confidence-Aware Unknown Activity Identification and Classification: We also design a confidence-aware supervised learning model and an adaptive cluster number K-means-based classification model to classify unknown activities.

• ***Unknown activity identification:*** In practice, known activities exhibit varied values in the confidence vector, with one value significantly higher than the others. In contrast, since unknown activities are not included in the training dataset, they tend to produce evenly distributed confidence values. Based on this analysis, we employ a supervised learning model to extract discriminative features from confidence vectors. A labeled dataset including confidence vectors from both known and unknown activities is used for model training. The trained model outputs the decision of whether a confidence vector represents an unknown activity.

• ***Unknown activity classification:*** An adaptive cluster number K-means-based classification model is designed to classify unknown activities recorded in the above-mentioned dataset into k groups. This raises the following two questions: **(i)** ***How to determine*** k***?*** **(ii)** ***How to update*** k ***dynamically when new unknown activities appear?***

To determine the cluster number k, we adopt the widely used elbow method [35]. First, the Sum-of-Squared Errors (SSE) of the dataset is calculated as $\text{SSE} = \sum_{i=1}^{K}\sum_{x\in D_i}\|x-\mu_i\|^2$, with D_i and μ_i representing i-th cluster and the centroid of cluster D_i, respectively. K denotes the upper limit of k and can be estimated through domain knowledge and prior information [36] or incremental testing [37]. By analyzing the rate of change in SSE as k increases, an elbow point can be identified, indicating the optimal cluster number k.

To answer the second question, an isolation forest model [38] is used to update k dynamically. Specifically, before classifying the unknown dataset, we combine the current received data with the existing unknown activity dataset and feed it into the isolation forest model. If the output is 1, it means that the currently received unknown activity belongs to an existing cluster. Meanwhile, if the output of the model is -1, it means a new unknown activity is observed and we need to increase k to $k+1$.

B. Adaptive Intelligent Control (AIC)

Since optical wireless communication can be easily blocked by human activities, to improve OWC reliability, we introduce a novel ***adaptive intelligent control (AIC)*** method to dynamically determine the optimal pulse width based on the H-HAR sensing results and transmission feedback. Intuitively, the reliability of OWC can be improved by using wider signal pulses. However, this solution will significantly reduce the communication throughput. To overcome this challenge, the goal of AIC is to determine the optimal pulse width that ensures reliable communication while maximizing throughput.

1) Fast Pulse Width Range Scanning: We first design a ***fast pulse width range scanning module*** to quickly determine a range of pulse width that can maintain ongoing communication when varying human activities occur. Specifically, according to the normal response time supported by commodity PD (receiver) [39], the current optical communication system can support various pulse widths.

According to this hardware feature, we define an available pulse width range L that can be supported by OPTICS hardware components. In AIC, L is evenly divided in N sub-pulse widths, which can be modeled as a sequence $S_L = \{\frac{L}{N}, \frac{2L}{N}, ..., L\}$ and the component in S_L can be denoted as a variable l. Then, at the sender side, we select each l in S_L for modulation while the receiver will record the data rates and bit error rates and send feedback to the sender. When the bit error rate reaches 0%, the corresponding l is identified as L_{max}. Concurrently, the pulse width within the

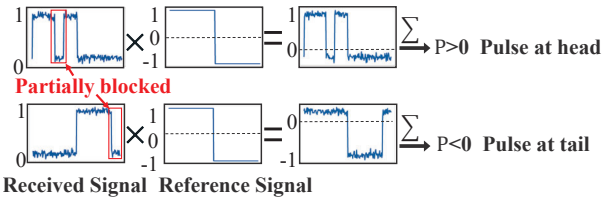

Fig. 8: Dynamic Pulse Demodulation

range from $\frac{L}{N}$ to L_{max} that achieves the highest data rate is set as L_{min}. The scanning process will continue until $L_{max} \neq L_{min}$. The final pulse width range $[L_{min}, L_{max}]$ will consist of pulse widths capable of maintaining acceptable communication during blockages. The parameter N is user-configurable to adjust scanning granularity and speed.

2) Optimal Pulse Width Determination: According to the calculated pulse width range $[L_{min}, L_{max}]$, we design an ***optimal pulse width determination module*** to find the optimal pulse width l^* by solving the following optimization problem:

$$\begin{aligned} \underset{l}{\text{Minimize}} \quad & R(l) = -\omega_1 f(l) + \omega_2 g(l) \\ \text{s.t.} \quad & f(l) = \frac{D}{l}, \quad g(l) = Q(\text{SNR}(l)), \\ & L_{min} \leq l \leq L_{max}, \end{aligned} \tag{1}$$

where $R(l)$ is the objective function to leverage the tradeoff between data rate and bit error rate requirements. $f(l)$ and $g(l)$ are functions for data rate and BER with respect to l, respectively. ω_1 and ω_2 are predefined weights according to the desired data rates or bit error rates. D is the duty cycle of the transmitted symbol. $Q(\text{SNR}(l))$ can be calculated as [40]:

$$Q(\text{SNR}(l)) = \frac{1}{2}\text{erfc}(\sqrt{\frac{\text{SNR}(l)}{2}}), \tag{2}$$

where erfc is the complementary error function, and $\text{SNR}(l)$ can be calculated as:

$$\text{SNR}(l) = \frac{lDP_{pulse}(1-\lambda)}{P_{noise}}. \tag{3}$$

P_{pulse} is the average received pulse power and P_{noise} is the noise power. λ is the average pulse blockage rate as illustrated in Figure 3 (b).

3) Pulse Width Range Adaptation: Due to the dynamic and unpredictable nature of human activity and varying environmental conditions, even the same activity performed by the same person can result in different optical signal patterns. Consequently, previously obtained pulse width range $[L_{min}, L_{max}]$ and optimal pulse l^* may become suboptimal or even unsuitable. A straightforward approach to tackle this problem is to repeat the fast pulse width range scanning process whenever the data or bit error rates cannot meet the user requirements. However, this approach is computationally intensive and can slow down the pulse width optimization process. In OPTICS, we design a ***pulse width range adaptation module*** to efficiently update the pulse width range.

To verify the suitability of the pulse width range $[L_{min}, L_{max}]$ for the ongoing activity, we define a reliability factor I, which can be calculated as $I = \omega_1 F - \omega_2 G$. F and G are data rates and bit error rates feedback from the receiver, respectively. ω_1 and ω_2 are the same coefficients as defined in (1). During the scanning process in the above Section IV-B1, OPTICS keeps recording the historical reliability factor I_{old}. When the same activity introduces signal blockage again, a new reliability factor I_{new} is obtained according to the current feedback from the receiver. We then compare I_{new} with I_{old} by computing $\Delta I = I_{new} - I_{old}$. If $\Delta I > 0$, we need to update the pulse width range. Otherwise, we can use the original pulse width. The updating mechanism is explained below:

- When $\omega_1 = 0$, we need to reduce bit error rates, indicating a larger L_{max} is needed. We need to iteratively increase the pulse width L_{max} by adding $\frac{L}{N}$ until $\Delta I < 0$ to find a new suitable upper bound of the pulse.
- When $\omega_2 = 0$, we need to increase data rates. Therefore, a smaller L_{min} is needed. To find the new L_{min}, we need to iteratively lower the current L_{min} by subtracting $\frac{L}{N}$ to find the first available pulse width such that $\Delta I < 0$.
- When $\omega_1 \neq 0$ & $\omega_2 \neq 0$, we need to adjust both L_{min} and L_{max}, where the above processes can be used.

C. Activity-Aware Dynamic & Adaptive Modulation/ Demodulation (ADAM)

To conduct dynamic modulation and demodulation based on pulses determined by the AIC, we design an ***activity-aware dynamic & adaptive modulation/demodulation (ADAM) module***. In ADAM, the modulation can be achieved by updating the pulse width. According to AIC, upon detecting signal blockage introduced by human activities, the pulse width is updated to the new l to ensure communication reliability.

However, demodulating the updated signal is challenging. As observed in Figure 4 (b), conventional VPPM demodulation struggles to accurately locate the pulse position to conduct demodulation, especially when the head or tail of the pulse symbol is blocked. To address this challenge, we design an innovative ***dynamic pulse demodulation module***. The **key idea** is to ***aggregate the power of the entire received symbol*** to determine the pulse position. Specifically, as shown in Figure 8, we first generate a reference signal r with a length of l, where the amplitude of the first half of r is 1 and the second half is -1. Then, we can compute the aggregate power level using $P = \sum_{t=1}^{l} |y(t)| * r(t)$, where y is the received signal power. $P > 0$ implies the pulse is located at the head of the symbol, while $P < 0$ means the pulse is located at the tail part of the symbol.

D. Blockage-Resilient Synchronization (BRS)

We have discussed how to sense human activities, determine the optimal pulse width according to the sensing results, and modulate and demodulate the optical signal accordingly. However, as the OPTICS transmitter dynamically changes the pulse width during transmission, we need to answer the following questions: ***How to inform the receiver about the updated pulse width?*** and ***How to conduct synchronization between sender and receiver?***

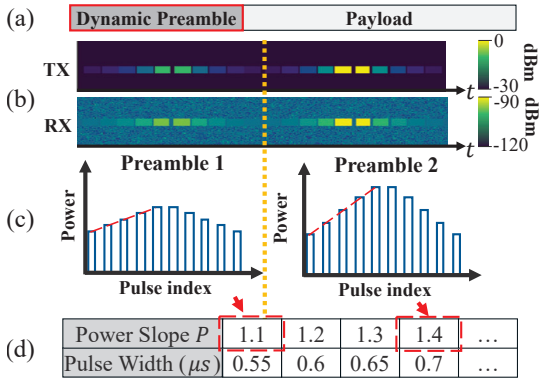

Fig. 9: OPTICS preamble: (a) OPTICS data packet consists of a dynamic preamble and a payload; (b) Spectrum diagram of two OPTICS preambles at transmitter and receiver; (c) The preamble consists of 10 pulses in total with transmission power increase/decrease linearly, and the changing rate is P; (d) Each pulse width has a unique preamble transmission power changing rate.

To answer these questions, our design is motivated by the observation in section II-C Figure 5 (b): although the receiver cannot successfully decode the received signal when disrupted, the PD can still detect the power variations in NLoS path signals. Based on this observation, we introduce an innovative ***blockage-resilient synchronization (BRS) module.*** The key idea is to dynamically change the preamble with varying power level pulses to inform the receiver about the updated pulse width and conduct synchronization simultaneously.

1) Dynamic Preamble Generation: The dynamic preamble consists of a sequence of equal-width pulse symbols with different power levels. As shown in Figure 9 (b) and (c), the structure of the preamble is symmetric, which consists of H pulses with linearly increasing transmission power and H pulses with decreasing transmission power. The absolute values of the slopes of these pulses are the same and are denoted as P. This design results in a **win-win outcome**: the receiver can easily synchronize to find the start position of the payload signal and simultaneously obtain the updated pulse width information needed for demodulation.

First, synchronization is achieved by identifying the peak pulse positions and using the slope to determine the start of the payload. The OPTICS receiver continuously monitors the presence and the received power of the preamble pulses. The symmetric structure of the preamble can help ensure robustness against channel variations. As shown in Figure 9 (b), the received power of the initial preamble pulse may be too low for reliable detection. If the preamble only includes pulses with linearly increasing transmission power, the receiver might misidentify the start of the payload due to the missed detection of the initial pulse(s). The parameter H is configurable and affects both detection reliability and system overhead, which can be determined according to user data rate requirements.

Second, to update the receiver with the changed pulse width for successful demodulation, we dynamically calculate P based on varying pulse width l using $P = \alpha l$. α is a scaling factor designed to ensure $P > 1$ and is pre-agreed upon by the transmitter and receiver. As shown in Figure 9 (d), each pulse width corresponds to a unique and distinct P, where α is set to 2. The receiver can first calculate P by using any two pulses within either the ascending or descending part in the received preamble, which is then used to calculate the current pulse width l. As OPTICS uses slope-related information P to calculate the updated pulse width, it allows the power level of the first pulse in the preamble to be adjusted according to channel conditions, thus ensuring robustness. Additionally, to prevent synchronization problems due to changes in pulse width, the pulse width in the preamble remains the same as the initially agreed l between the transmitter and the receiver.

Ideally, a preamble that consists of pulses with transmission power first linearly decreasing and then increasing can also conduct the synchronization. However, since the response time of different LED and PD varies [39], [41], immediate transmission power level change at the start of the preamble can lead to an unintended pulse power, which will result in the synchronization failure. In contrast, the beginning of our proposed preamble smoothly increases the transmission power, thus avoiding this problem.

2) Payload & Parameter Synchronization: The proposed payload & parameter synchronization module continuously monitors incoming optical signals to detect the preamble by identifying any linear variations in the received signal power. Once a potential preamble is detected, we use the least squares method to analyze the changes in the received signal power and confirm the presence of the preamble. We then identify the peak pulse in the preamble to determine the start of the payload based on pulse number H. Meanwhile, the pulse width is obtained by calculating $\frac{P_{front}+(-P_{back})}{2\alpha}$, where P_{front} and P_{back} are the power slopes of the first and second halves of the received preamble, respectively. After determining the start position of the payload as well as the pulse width, the receiver can demodulate the payload using the dynamic pulse demodulation module.

V. Implementation and Evaluation

A. OPTICS Implementation

• **Implementation Details.** We implement the transmitter of OPTICS using USRP N210 with daughter board LFTX [42], an operational amplifier ZX60-100VH+, a bias-tee ZFBT-4R2GW-FT+, and a Thorlabs MWWHD4 LED light bulb [43]. Specifically, the USRP is connected to a laptop to support real-time data processing. The operational amplifier and the bias-tee are used to amplify the output voltage signal from N210 and ensure that the voltage fed to the light source is non-negative. The operating power of the LED light bulb is $8488mW$. The color temperature is $3000K$ and the field of view is $135°$, which follows the LED standard in normal indoor scenarios [44].

The OPTICS receiver is implemented using USRP N210 with an LFRX daughter board. We use a Thorlabs PDA100A2 [45] with a field of view $165°$ to implement the receiver frontend (PD). This PD can detect light within a wavelength ranging from $320nm$ to $1100nm$.

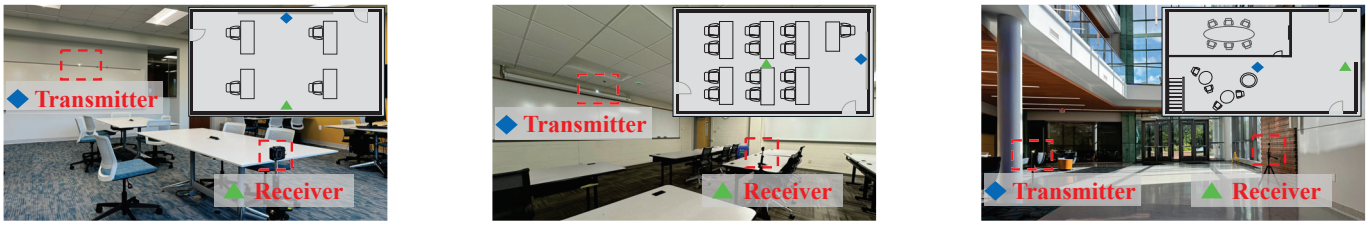

(a) Lab Scenario (b) Classroom Scenario (c) Lobby Lounge Scenario

Fig. 10: Evaluation Setup in Lab, Classroom, and Lobby Lounge Scenarios

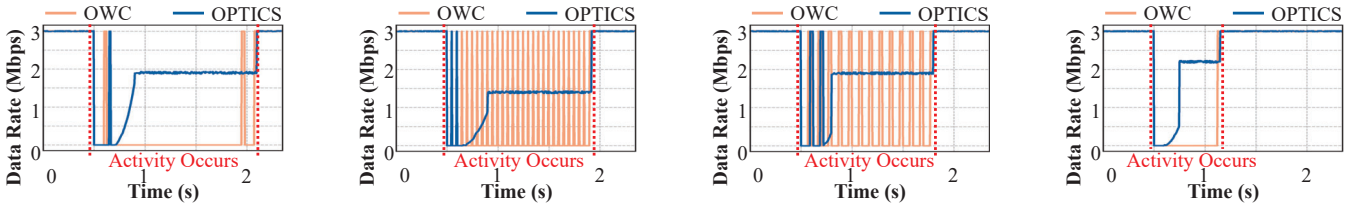

(a) Walking (b) Waving Arm (c) Kicking (d) Running

Fig. 11: Data Rates vs. Different Activities

Accuracy (%)	Walk	Wave	Kick	Run
Lab	98.1	99.1	98.7	95.7
Classroom	97.6	98.4	98.2	94.2
Lobby	97.3	97.9	97.3	94.8

TABLE II: Known Activity Recognition Accuracy

Accuracy(%)	Spin	Punch	Dance	Shake
Lab	97.1	97.7	96.4	95.8
Classroom	96.7	96.9	95.6	95.4
Lobby	96.2	95.1	94.7	94.3

TABLE III: Unknown Activity Classification Accuracy

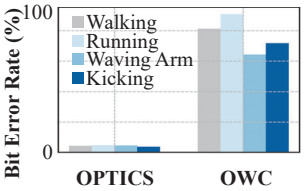

Fig. 12: Bit Error Rate vs. Different Activities

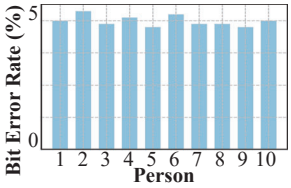

Fig. 13: Bit Error Rate vs. Different Individuals

• **Evaluation Scenarios.** As shown in Figure 10, we extensively evaluate the performance of OPTICS in different scenarios, including the lab, classroom, and lobby lounge. The distances between the transmitter and receiver are $6m$ (lab), $8m$ (classroom), and $10m$ (lobby lounge). We have 10 volunteers to perform activities for the evaluation of OPTICS. The heights of the volunteers range from $165cm$ to $195cm$. We collected 10000 samples to train the proposed H-HAR model, including four known activities (i.e., walking, waving arms, kicking, and running) and four unknown activities (i.e., spinning, throwing punches, dancing, and shaking hands).

B. Evaluation Results

1) Sensing Evaluation: We first study the sensing accuracy of OPTICS in Table II and Table III. As shown in Table II, the activity recognition accuracy can be as high as 99.1% in the lab scenario. Even in the worst case (lobby lounge scenario), the average activity recognition accuracy is still around 97%. In Table III, we study the performance of OPTICS when unknown activities occur. This experiment is very challenging since our system has never been trained to classify these activities. However, in the lab and classroom scenarios, the average activity classification accuracy is higher than 96%, which demonstrates the effectiveness of our H-HAR model. Even in the lobby lounge scenario, the average activity classification accuracy is still higher than 95%. We also want to emphasize that the light conditions in the lobby lounge scenario are extremely complex. However, instead of using raw optics signals for sensing, OPTICS leverages the received data bits to perform activity recognition and classification, which significantly improves the system's robustness. **In summary**, OPTICS can achieve high-accuracy activity recognition and classification in various scenarios.

2) Communication Evaluation: We also study the communication performance of OPTICS when the signal is dynamically blocked by human activities. Since the evaluation results and trends are similar in different scenarios, in this subsection, we only show the experiment results in the lab scenario.

• **Data Rate and Bit Error Rate.** Figures 11 and 12 show the data rate and bit error rate of OPTICS. Since this is the first work that seamlessly integrates OWC and optical sensing to create a win-win situation, the state-of-the-art is complimentary, however, provides no appropriate baselines for comparison. To directly show the advantages of OPTICS, we use the traditional OWC system as the comparison.

As depicted in Figure 11, OPTICS and the traditional OWC can achieve the same data rate when the communication path is not blocked. However, when human activities occur, the traditional OWC system suffers extremely severe data rate fluctuations and the data rates reduce to $0Mbps$. In contrast, since OPTICS utilizes Adaptive Intelligent Control (AIC) to dynamically adjust the communication signal according to the sensing results, it can preserve the original communication without significantly sacrificing the data rate.

Figure 12 compares the bit error rate between OPTICS and OWC when human activities occur. As we can see from this figure, the bit error rate of OWC is much higher than that of OPTICS. The average bit error rate of OWC is around 77.125%, which is almost 17.93 times as high as that of OPTICS (4.3%). This result further proves that our system can maintain reliable communication during blockage.

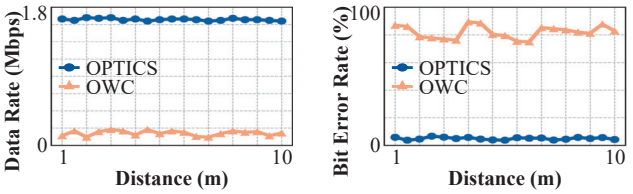

(a) Data Rate vs. Distance (b) Bit Error Rate vs. Distance

Fig. 14: Transmission Distance (Lab Scenario)

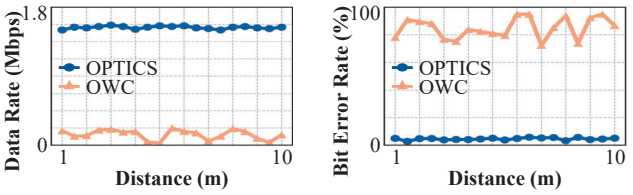

(a) Data Rate vs. Distance (b) Bit Error Rate vs. Distance

Fig. 15: Transmission Distance (Lobby Lounge Scenario)

• **Adaptability of OPTICS.** We also study the impacts of the same activity performed by different individuals. Since the evaluation results show similar trends, Figure 13 shows the bit error rate when different individuals are walking between the transmitter and receiver. The bit error rate is very stable regardless of the activities generated by different people. This is because the Adaptive Intelligent Control (AIC) in OPTICS can dynamically adjust the communication signal to ensure communication reliability. **In summary**, OPTICS can support reliable and high-speed communication when the signal is blocked by human activities.

3) Transmission Distance: We also study the impacts of transmission distance on OPTICS in Figures 14 and 15. As shown in Figure 14, in the lab scenario, the data rate of OPTICS is very stable (around $1.72Mbps$) and the corresponding bit error rate is almost 0. In contrast, the traditional OWC system cannot even conduct communication. In Figure 15, the performance of OPTICS is only slightly decreased. This is because the lobby lounge has extremely complex light illumination conditions. Although OPTICS can dynamically adjust the transmitted optical signal according to human activities, the random ambient light signals still slightly affect the received signal. However, even in this worst scenario, our system is still able to achieve a $1.68Mbps$ data rate, which demonstrates the effectiveness of our design. **In summary**, OPTICS can support reliable and high-throughput communication regardless of communication distances.

4) Long-Term Evaluation: In Figures 16 and 17, we show the results of long-term experiments conducted over one month to fully study the effectiveness of OPTICS and demonstrate the significant advantages of our design over traditional OWC systems. In these scenarios, we did not control the number of people crossing the path between the transmitter and receiver. Since the results were highly similar each day, we show the results for one representative day. As shown in these figures, during crowded hours, the traditional OWC system suffers significant performance degradation in both lab and lobby lounge scenarios. On the contrary, OPTICS can achieve stable communication with very low bit error rates. We also can observe that human activities will frequently

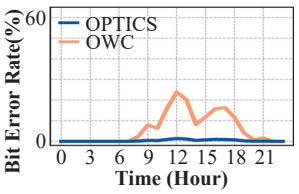

Fig. 16: Bit Error Rate (Lab Scenario)

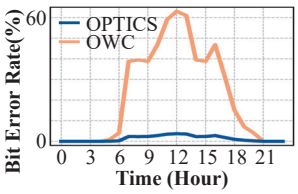

Fig. 17: Bit Error Rate (Lobby Lounge Scenario)

block optical communication in real-world scenarios, which necessitates the urgent implementation of OPTICS to support reliable and high-throughput optical communication in these environments.

VI. Related Work

Optical Wireless Communication. In recent years, we have witnessed an increasing number of works [20]–[22] focused on enhancing the reliability of OWC to address the communication disruption issues caused by blockage. In [20], the author proposes an OWC system using mirror array-based RIS along the transmission path and an LC-based RIS OWC receiver to address the blockage issues. RIS demonstrates promising performance, while the expensive components and professional installation requirements prevent RIS from being a widely adopted approach in practical scenarios.

Wireless Sensing. Wireless sensing has been envisioned as a promising technology for capturing information about human targets [46], [47]. Several works have been introduced to conduct optical-based wireless sensing [32], [33]. For example, in Aili [33] and Starlight [32], they leverage PD arrays and LED panels to capture and analyze the 2D projection shadow from the human body, achieving accurate human activity recognition. These approaches can achieve high activity recognition accuracy and have the potential to be widely adopted in real-world scenarios.

Different from these approaches, OPTICS seamlessly integrates sensing and communication to create a win-win situation for both sensing and communication tasks. It can significantly improve communication reliability and speed while conducting human activity recognition at the same time.

VII. Conclusion

In this work, we propose OPTICS, the first system that seamlessly integrates both optical wireless communication and sensing. By analyzing the received data pattern, OPTICS can precisely identify the human activities that cause the optical signal blockage and dynamically determine the optimal pulse width to preserve communication. We implemented OPTICS using off-the-shelf products and conducted extensive evaluations under various real-world scenarios. Our evaluation results show that OPTICS can achieve reliable and high-throughput communication while also achieving accurate human activity recognition. It opens a new direction to support future communication-for-sensing and sensing-for-communication research.

Acknowledgment

This work is partially supported by NSF grants CCF-2347888.

REFERENCES

[1] P. H. Pathak, X. Feng, P. Hu, and P. Mohapatra, "Visible Light Communication, Networking, and Sensing: A Survey, Potential and Challenges," *IEEE Communications Surveys & Tutorials*, 2015.

[2] M. Z. Chowdhury, M. K. Hasan, M. Shahjalal, M. T. Hossan, and Y. M. Jang, "Optical wireless hybrid networks: Trends, opportunities, challenges, and research directions," *IEEE Communications Surveys & Tutorials*, 2020.

[3] I. F. Akyildiz, A. Kak, and S. Nie, "6g and beyond: The future of wireless communications systems," *IEEE access*, 2020.

[4] F. Wang, F. Yang, J. Song, and Z. Han, "Access Frameworks and Application Scenarios for Hybrid VLC and RF Systems: State of the Art, Challenges, and Trends," *IEEE Communications Magazine*, vol. 60, no. 3, pp. 55–61, 2022.

[5] Y. Zhang and N. Cen, "Programmable Software-Defined Testbed for Visible Light UAV Networks: Architecture Design and Implementation," in *In Proc. Of Consumer Communications Networking Conference (CCNC)*, Las Vegas, NV, USA, 2023.

[6] Y. Zhang and N. Cen, "Countering RF Side-Channel Sniffing in Optical Wireless Communication," in *In Proc. of IEEE International Conference on Communications (ICC)*, Denver, CO, USA, 2024.

[7] A. Kaba, S. Sahuguede, and A. Julien-Vergonjanne, "Channel modeling of an optical wireless body sensor network for walk monitoring of elderly," *Sensors*.

[8] O. Haddad, M.-A. Khalighi, S. Zvanovec, and M. Adel, "Channel characterization and modeling for optical wireless body-area networks," *IEEE Open Journal of the Communications Society*, 2020.

[9] B. Donmez, R. Mitra, and F. Miramirkhani, "Channel modeling and characterization for vlc-based medical body sensor networks: trends and challenges," *IEEE Access*, 2021.

[10] J. Li, X. Bao, and W. Zhang, "LED adaptive deployment optimization in indoor VLC networks," *China Communications*, vol. 18, no. 6, pp. 201–213, 2021.

[11] I. N'doye, D. Zhang, M.-S. Alouini, and T.-M. Laleg-Kirati, "Establishing and maintaining a reliable optical wireless communication in underwater environment," *IEEE Access*, 2021.

[12] X. Liu, W. Wang, G. Song, and T. Zhu, "{LightThief}: Your optical communication information is stolen behind the wall," in *32nd USENIX Security Symposium (USENIX Security 23)*, 2023.

[13] T. Li, Q. Liu, and X. Zhou, "Practical Human Sensing in the Light," in *In Proc. of the Annual International Conference on Mobile Systems, Applications, and Services (MobiSys)*, MobiSys '16, Singapore, Singapore, 2016.

[14] L. Shi, Z. Liu, B. Béchadergue, H. Guan, L. Chassagne, and X. Zhang, "Experimental demonstration of integrated optical wireless sensing and communication," *Journal of Lightwave Technology*, 2024.

[15] A. M. Abdelhady, O. Amin, M.-S. Alouini, and B. Shihada, "Revolutionizing optical wireless communications via smart optics," *IEEE Open Journal of the Communications Society*, 2022.

[16] S. R. Teli, S. Zvanovec, and Z. Ghassemlooy, "Optical internet of things within 5g: Applications and challenges," in *2018 IEEE International Conference on Internet of Things and Intelligence System (IOTAIS)*, 2018.

[17] A. Celik, I. Romdhane, G. Kaddoum, and A. M. Eltawil, "A top-down survey on optical wireless communications for the internet of things," *IEEE Communications Surveys & Tutorials*, 2022.

[18] H. B. Eldeeb, S. Naser, L. Bariah, S. Muhaidat, and M. Uysal, "Digital twin-assisted owc: Towards smart and autonomous 6g networks," *IEEE Network*, 2024.

[19] X. Huang, X. Pan, Z. Wan, M. Xu, Z. Wang, X. Liu, Y. Wang, and X. Zhang, "A novel experimental visible light positioning system with low bandwidth requirement and high precision pulse reconstruction," in *2023 13th International Conference on Indoor Positioning and Indoor Navigation (IPIN)*, 2023.

[20] O. Maraqa and T. M. N. Ngatched, "Optimized Design of Joint Mirror Array and Liquid Crystal-Based RIS-Aided VLC Systems," *IEEE Photonics Journal*, 2023.

[21] D. Sabui, S. Chatterjee, and G. S. Khan, "Impact of different receiver geometries on a reconfigurable intelligent surface assisted multi-cell VLC system in the presence of light path blockage," *Appl. Opt.*, 2024.

[22] B. Cao, M. Chen, Z. Yang, M. Zhang, J. Zhao, and M. Chen, "Reflecting the Light: Energy Efficient Visible Light Communication with Reconfigurable Intelligent Surface," in *Proc. of IEEE Vehicular Technology Conference*, Victoria, Canada, November 2020.

[23] T. Li, Q. Liu, and X. Zhou, "Practical human sensing in the light," in *Proceedings of the 14th Annual International Conference on Mobile Systems, Applications, and Services*, 2016.

[24] M. Pang, G. Shen, X. Yang, K. Zhang, P. Chen, and G. Wang, "Achieving reliable underground positioning with visible light," *IEEE Transactions on Instrumentation and Measurement*, 2022.

[25] D. Ma, G. Lan, C. Hu, M. Hassan, W. Hu, M. B. Upama, A. Uddin, and M. Youssef, "Recognizing hand gestures using solar cells," *IEEE Transactions on Mobile Computing*, 2022.

[26] Z. Liao, Z. Luo, Q. Huang, L. Zhang, F. Wu, Q. Zhang, and G. Chen, "Gesture recognition using visible light on mobile devices," *IEEE/ACM Transactions on Networking*, 2024.

[27] J.-H. Yoo and S.-Y. Jung, "Modeling and analysis of variable ppm for visible light communications," *EURASIP Journal on Wireless Communications and Networking*, 2013.

[28] J. Zhang, F. Wu, B. Wei, Q. Zhang, H. Huang, S. W. Shah, and J. Cheng, "Data augmentation and dense-lstm for human activity recognition using wifi signal," *IEEE Internet of Things Journal*, 2020.

[29] B. Fu, N. Damer, F. Kirchbuchner, and A. Kuijper, "Sensing technology for human activity recognition: A comprehensive survey," *IEEE Access*, 2020.

[30] R. Gao, M. Zhang, J. Zhang, Y. Li, E. Yi, D. Wu, L. Wang, and D. Zhang, "Towards position-independent sensing for gesture recognition with wi-fi," *Proceedings of the ACM on Interactive, Mobile, Wearable and Ubiquitous Technologies*, 2021.

[31] F. Demrozi, G. Pravadelli, A. Bihorac, and P. Rashidi, "Human activity recognition using inertial, physiological and environmental sensors: A comprehensive survey," *IEEE access*, 2020.

[32] T. Li, Q. Liu, and X. Zhou, "Practical Human Sensing in the Light," in *In Proc. of the Annual International Conference on Mobile Systems, Applications, and Services (MobiSys)*, Singapore, Singapore, 2016.

[33] T. Li, X. Xiong, Y. Xie, G. Hito, X.-D. Yang, and X. Zhou, "Reconstructing Hand Poses Using Visible Light," *Proc. ACM Interact. Mob. Wearable Ubiquitous Technol.*, vol. 1, no. 3, 2017.

[34] V. Mariappan and J. Cha, "Ieee802. 15.7 m owc phy specification overview," *IEEE COMSOC MMTC Commun. Front*, 2018.

[35] E. Umargono, J. E. Suseno, and S. V. Gunawan, "K-Means Clustering Optimization Using the Elbow Method and Early Centroid Determination Based on Mean and Median Formula," in *Proceedings of the 2nd International Seminar on Science and Technology (ISSTEC 2019)*, 2020.

[36] M. Shi, J. Liu, B. Cao, Y. Wen, and X. Zhang, "A Prior Knowledge Based Approach to Improving Accuracy of Web Services Clustering," in *IEEE International Conference on Services Computing (SCC)*, 2018.

[37] A. Abernathy and M. E. Celebi, "The incremental online k-means clustering algorithm and its application to color quantization," *Expert Systems with Applications*, 2022.

[38] R. Alsini, A. Almakrab, A. Ibrahim, and X. Ma, "Improving the outlier detection method in concrete mix design by combining the isolation forest and local outlier factor," *Construction and Building Materials*, 2021.

[39] Thorlabs, 2024. https://www.thorlabs.com/images/TabImages/Noise_Equivalent_Power_White_Paper.pdf.

[40] M. D. Audeh, J. M. Kahn, and J. R. Barry, "Performance of pulse-position modulation on measured non-directed indoor infrared channels," *IEEE Transactions on Communications*, 1996.

[41] L. Svilainis, "LED PWM dimming linearity investigation," *Displays*, 2008.

[42] Ettus, 2024. https://www.ettus.com/all-products/un210-kit/.

[43] Thorlabs, 2024. https://www.thorlabs.com/thorproduct.cfm?partnumber=MWWHD4.

[44] WAC Lighting, 2024. https://www.minicircuits.com/WebStore/dashboard.html?model=ZFBT-4R2GW-FT%2B.

[45] Thorlabs, 2024. https://www.thorlabs.com/thorproduct.cfm?partnumber=PDA100A2.

[46] B. Xie, M. Cui, D. Ganesan, X. Chen, and J. Xiong, "Boosting the Long Range Sensing Potential of LoRa," in *Proceedings of the 21st Annual International Conference on Mobile Systems, Applications and Services*, 2023.

[47] M. Cui, B. Xie, Q. Wang, and J. Xiong, *DancingAnt: Body-empowered Wireless Sensing Utilizing Pervasive Radiations from Powerline*. 2023.